DTIC FILE COPY

AD-A218 622

Defense Nuclear Agency
Alexandria, VA 22310-3398

DNA-TR-89-76

Preliminary Results of the Peak Experiment
ALTAIR Deep-Space Measurements

D. L. Knepp
Mission Research Corporation
P.O. Box 51203
Pacific Grove, CA 93950-6203

March 1990

Technical Report

CONTRACT No. DNA 001-87-C-0169

Approved for public release;
distribution is unlimited.

DTIC
ELECTE
MAR 05 1990
S B D

90 03 02 088

Destroy this report when it is no longer needed. Do not return to sender.

PLEASE NOTIFY THE DEFENSE NUCLEAR AGENCY, ATTN: CSTI, 6801 TELEGRAPH ROAD, ALEXANDRIA, VA 22310-3398, IF YOUR ADDRESS IS INCORRECT, IF YOU WISH IT DELETED FROM THE DISTRIBUTION LIST, OR IF THE ADDRESSEE IS NO LONGER EMPLOYED BY YOUR ORGANIZATION.

DISTRIBUTION LIST UPDATE

This mailer is provided to enable DNA to maintain current distribution lists for reports. We would appreciate your providing the requested information.

- ☐ Add the individual listed to your distribution list.
- ☐ Delete the cited organization/individual.
- ☐ Change of address.

NAME: _____

ORGANIZATION: _____

OLD ADDRESS	CURRENT ADDRESS
_____	_____
_____	_____
_____	_____

TELEPHONE NUMBER: (___) _____

SUBJECT AREA(s) OF INTEREST:

_____	_____
_____	_____
_____	_____

DNA OR OTHER GOVERNMENT CONTRACT NUMBER: _____

CERTIFICATION OF NEED-TO-KNOW BY GOVERNMENT SPONSOR (if other than DNA):

SPONSORING ORGANIZATION: _____

CONTRACTING OFFICER OR REPRESENTATIVE: _____

SIGNATURE: _____

CUT HERE AND RETURN

Director
Defense Nuclear Agency
ATTN: TITL
Washington, DC 20305-1000

Director
Defense Nuclear Agency
ATTN: TITL
Washington, DC 20305-1000

UNCLASSIFIED
SECURITY CLASSIFICATION OF THIS PAGE

REPORT DOCUMENTATION PAGE

1a REPORT SECURITY CLASSIFICATION UNCLASSIFIED	1b RESTRICTIVE MARKINGS
2a SECURITY CLASSIFICATION AUTHORITY N/A since Unclassified	3. DISTRIBUTION/AVAILABILITY OF REPORT Approved for public release; distribution is unlimited.
2b DECLASSIFICATION/DOWNGRADING SCHEDULE N/A since Unclassified	
4 PERFORMING ORGANIZATION REPORT NUMBER(S) MRC/MRY-R-014	5. MONITORING ORGANIZATION REPORT NUMBER(S) DNA-TR-89-76
6a NAME OF PERFORMING ORGANIZATION Mission Research Corporation 6b OFFICE SYMBOL (if applicable)	7a NAME OF MONITORING ORGANIZATION Defense Nuclear Agency
6c ADDRESS (City, State, and ZIP Code) P.O. Box 51203 Pacific Grove, CA 93950-6203	7.b. ADDRESS (City, State, and ZIP Code) 6801 Telegraph Road Alexandria, Va 22310-3398
8a NAME OF FUNDING/SPONSORING ORGANIZATION 8b OFFICE SYMBOL (if applicable) RAAE/Schrock	9 PROCUREMENT INSTRUMENT IDENTIFICATION NUMBER DNA 001-87-C-0169
8c ADDRESS (City, State, and ZIP Code)	10. SOURCE OF FUNDING NUMBERS PROGRAM ELEMENT NO. 62715H; PROJECT NO. RB; TASK NO. RB; WORK UNIT ACCESSION NO. DH870169

11 TITLE (Include Security Classification)
Preliminary Results of the Peak Experiment
ALTAIR Deep-Space Measurements

12 PERSONAL AUTHOR(S)
Knepp, Dennis L.

13a TYPE OF REPORT	13b TIME COVERED	14 DATE OF REPORT (Year, Month, Day)	15 PAGE COUNT
Technical	FROM 870827 TO 890306	900301	40

16 SUPPLEMENTARY NOTATION
This work was sponsored by the Defense Nuclear Agency under RDT&E RMC Codes B466D RB RB 0P140 25904D, B466D RB RB EA104 25904D, and B466D RB RB 00140 25904D.

17 COSATI CODES		
FIELD	GROUP	SUB-GROUP
22	2	cont'd
20	14	

18 SUBJECT TERMS (Continue on reverse if necessary and identify by block number)
ALTAIR; FLTSATCOM; PEAK Experiment; Scintillation; (KT); Radio Wave Propagation;

19 ABSTRACT (Continue on reverse if necessary and identify by block number)

During the DNA PEAK (Propagation Effects Assessment-Kwajalein) experiment in August 1988, the primary use of ALTAIR consisted of the collection of VHF and UHF track data and pulse returns from low-orbiting spherical satellites and other satellites of opportunity. However during the course of the experiment the opportunity occurred to collect a small amount of data while ALTAIR was in its operational deep-space track mode. This brief report summarizes the deep-space track data collected by ALTAIR on the evenings of August 18 and 19. On both evenings the FLTSATCOM 4 satellite was tracked by ALTAIR for a brief period. Simultaneous measurements of the one-way signal from the FLTSATCOM UHF satellite beacon at 244 MHz were also obtained at a receiver site located on Roi-Namur.

A comparison of the ALTAIR data collected from the two-way radar propagation path to the FLTSATCOM satellite versus the one-way satellite link data indicates that, during this brief period, ALTAIR experienced about 5 dB of loss in detection sensitivity. Although

20 DISTRIBUTION AVAILABILITY OF ABSTRACT ☐ UNCLASSIFIED UNLIMITED ☒ SAME AS REPORT ☐ DTIC USERS	21 ABSTRACT SECURITY CLASSIFICATION UNCLASSIFIED
22a NAME OF RESPONSIBLE INDIVIDUAL Bennie F. Maddox	22b TELEPHONE (Include Area Code) (703) 325-7042 22c OFFICE SYMBOL DNA/CSTI

DD FORM 1473, JUN 86 Previous editions are obsolete

SECURITY CLASSIFICATION OF THIS PAGE
UNCLASSIFIED

19. ABSTRACT (Continued)

this loss does indeed degrade ALTAIR deep-space detection and track functions, it has little effect on ALTAIR operational performance of its mission to update the national NORAD data base of space objects. This statement is a consequence of the fact that deep-space track updates are required only on a weekly basis, and any individual track update may easily be postponed until more favorable propagation conditions prevail. However, if ALTAIR were faced with time-critical deep-space track requirements, mitigation techniques would likely be required to combat the effects of severe equatorial scintillation. Keywords: previous page

Accession For	
NTIS GRA&I	☑
DTIC TAB	☐
Unannounced	☐
Justification	
By	
Distribution/	
Availability Codes	
Dist	Avail and/or Special
A-1	

QUALITY INSPECTED 4

CONVERSION TABLE

Conversion factors for U.S. Customary to metric (SI) units of measurement

MULTIPLY →	BY →	TO GET
TO GET ←	BY ←	MULTIPLY
angstrom	1.000000 x E -10	meters (m)
atmosphere (normal)	1.01325 x E +2	kilo pascal (kPa)
bar	1.000000 x E +2	kilo pascal (kPa)
barn	1.000000 x E -28	meter^2 (m^2)
British thermal unit (thermochemical)	1.054350 x E +3	joule (J)
calorie (thermochemical)	4.184000	joule (J)
cal (thermochemical) / cm^2	4.184000 x E -2	mega joule/m^2 (MJ/m^2)
curie	3.700000 x E +1	*giga becquerel (GBq)
degree (angle)	1.745329 x E -2	radian (rad)
degree Farenheit	$(t_K=t_F+459.67)/1.8$	degree kelvin (K)
electron volt	1.60219 x E -19	joule (J)
erg	1.000000 x E -7	joule (J)
erg/second	1.000000 x E -7	watt (W)
foot	3.048000 x E -1	meter (m)
foot-pound-force	1.355818	joule (J)
gallon (U.S. liquid)	3.785412 x E -3	meter^3 (m^3)
inch	2.540000 x E -2	meter (m)
jerk	1.000000 x E +9	joule (J)
joule/kilogram (J/kg) (radiation dose absorbed)	1.000000	Gray (Gy)
kilotons	4.183	terajoules
kip (1000 lbf)	4.448222 x E +3	newton (N)
kip/inch^2 (ksi)	6.894757 x E +3	kilo pascal (kPa)
ktap	1.000000 x E +2	newton-second/m^2 (N-s/m^2)
micron	1.000000 x E -6	meter (m)
mil	2.540000 x E -5	meter (m)
mile(international)	1.609344 x E +3	meter (m)
ounce	2.834952 x E -2	kilogram (kg)
pound-force (lbs avoirdupois)	4.448222	newton (N)
pound-force inch	1.129848 x E -1	newton-meter (N·m)
pound-force/inch	1.751268 x E +2	newton/meter (N/m)
pound-force/foot^2	4.788026 x E -2	kilo pascal (kPa)
pound-force/inch^2 (psi)	6.894757	kilo pascal (kPa)
pound-mass (lbm avoirdupois)	4.535924 x E -1	kilogram (kg)
pound-mass-foot^2 (moment of inertia)	4.214011 x E -2	kilogram-meter^2 (kg·m^2)
pound-mass/foot^3	1.601846 x E +1	kilogram/meter^3 (kg/m^3)
rad (radiation dose absorbed)	1.000000 x E -2	**Gray (Gy)
roentgen	2.579760 x E -4	coulomb/kilogram (C/kg)
shake	1.000000 x E -8	second (s)
slug	1.459390 x E +1	kilogram (kg)
torr (mm Hg, 0° C)	1.333220 x E -1	kilo pascal (kPa)

*The becquerel (Bq) is the SI unit of radioactivity; 1 Bq = 1 event/s.
**The Gray (Gy) is the SI unit of absorbed radiation.

TABLE OF CONTENTS

LIST OF ILLUSTRATIONS

LIST OF ILLUSTRATIONS (Continued)

SECTION 1

INTRODUCTION

This report describes the deep-space portion of the DNA August 1988 Propagation Effects Assessment Experiment that took place at the Kwajalein Atoll in the Marshall Islands. Starting on August 1, a four week campaign was accomplished during which time many satellite passes were observed using the ALTAIR VHF and UHF wide bandwidth waveforms.

The primary experiment involved the use of the ALTAIR VHF and UHF waveforms to track spherical satellites and other satellites of opportunity in an effort to observe severe signal scintillation due to ionospheric F-region structure. The key objective of the experiment was to determine the effect of scintillation on the radar measurement functions including radar track, target amplitude and phase measurement, and radar doppler processing capability. The results of these radar measurements will be correlated with the observed state of the ionosphere obtained from other measurements including radar backscatter measurements and satellite beacon experiments. The ultimate goal of the PEAK program is to correlate the radar performance measurements with ionospheric structure measurements in order to facilitate radar performance prediction when the ionosphere is disturbed by high-altitude nuclear detonations. The data base obtained from the DNA PEAK experiment will also provide actual measurements of radar performance against which simulations and predictions can be compared for verification.

Together with the primary experiment, two other categories of experiment involving other sensors were accomplished. The two categories are (1) one-way and two-way propagation measurements along the same path, and (2) various diagnostic measurements of the disturbed ionosphere. The goal of the first category was to relate the observed one-way and two-way signal statistics and thereby verify theoretical results. Analysis of this data is continuing. The major purpose for diagnostic support was to provide a predictive capability for disturbed ionospheric conditions in real time so that we could optimize our scintillation measurement opportunities.

SECTION 2

DEEP-SPACE TRACK SUMMARY

In the operational ALTAIR deep-space mode, targets at very long ranges are tracked at UHF for brief periods of time to obtain metric information to update the national data base of satellite orbit information. The data obtained from ALTAIR during the PEAK experiment utilized a 400 μ-second duration linear frequency modulated pulse with a chirping bandwidth of 250 kHz. This waveform gives a 6 dB range resolution of 1100 m and was transmitted at a maximum pulse repetition frequency of 120 Hz at a peak power of 4.5 megawatts.

Upon reception, a coherent pulse-train comprising 512 (or more depending on signal-to-noise ratio after integration) pulses is coherently integrated, the peak doppler is tracked and the satellite position is determined. Typically 512 pulses are integrated using a total of 108 range gates to locate the target in both range and doppler.

Figures 1 and 2 give examples of the video display that is available to the operators at ALTAIR to enable them to control the radar. The top portion of e figure shows the value of received power as a function of range over a range about 50 km. This plot is obtained by summing the returns in all the dopp each range bin. The range extent shown in Figure 1 lies between 35928 and 3 in Figure 2 the range extent ranges from 35978 to 35999 km. The ordinate scale upper portion of each figure shows the signal-to-noise ratio in units of decibels from zero to 30 dB. The lower portion of each figure shows the received signal spectrum versus doppler frequency from -58 to 58 Hz. This plot shows the doppler spectrum of the single range bin that contains the maximum power. Note that the target dopple has been tracked so that the principal return appears at zero doppler in the plot.

Both figures show data taken about a week apart from the FLTSATCOM 4 satellite located in synchronous orbit at 172° East longitude. The data displayed in Figure 1 is taken during a period of little ionospheric activity where the received SNR, after integration, is relatively high. In Figure 2 fading reduces the received SNR so that the satellite return is no longer discernable on this particular plot. These two figures are included in this report as examples of how scintillation appears on the displays that are used by ALTAIR operators.

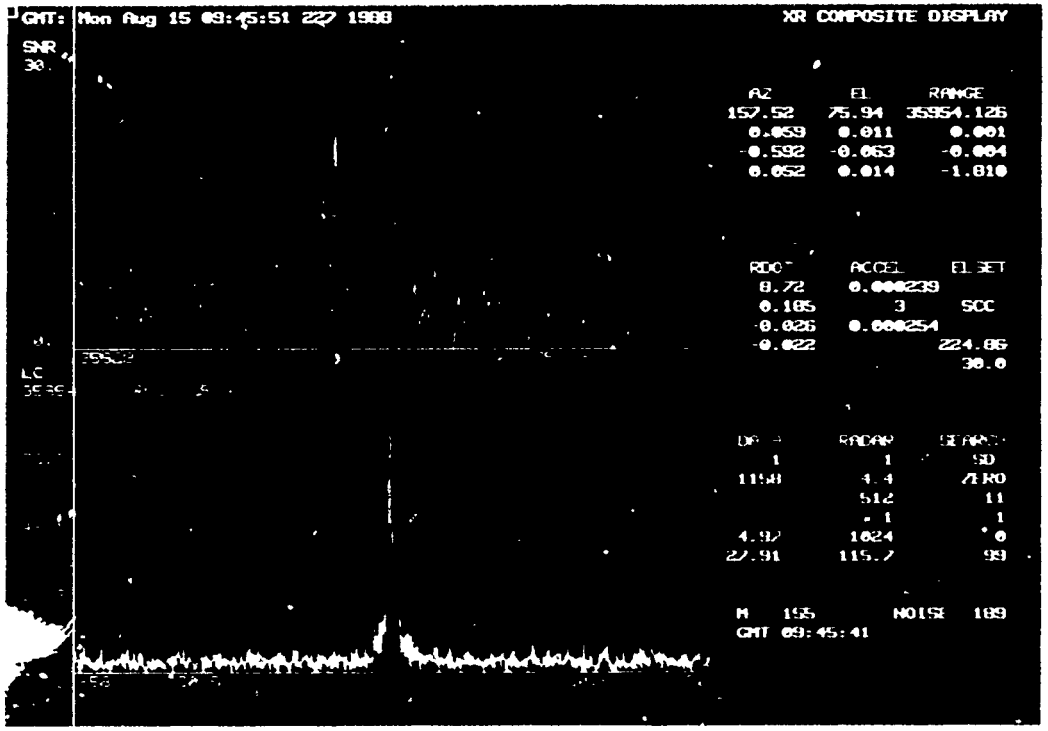

Figure 1. Example of the ALTAIR console display on GMT day 227, 1988 showing received pulse shape after integration (top) and doppler spectrum (bottom) during a period of little ionospheric activity.

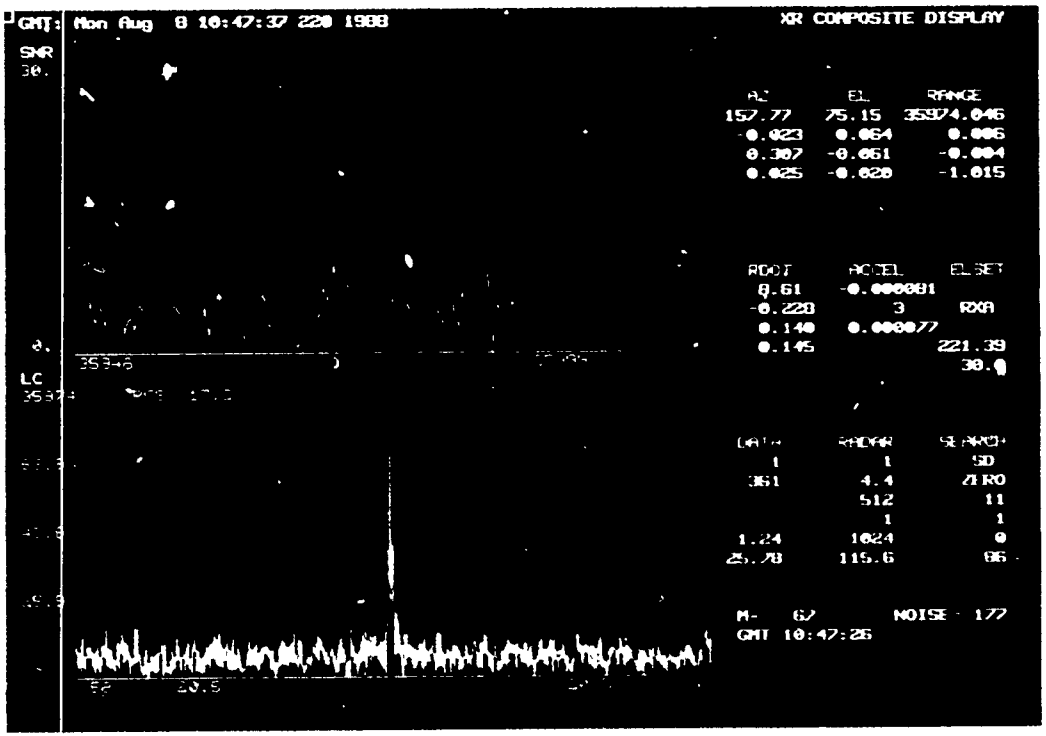

Figure 2. Example of the ALTAIR console display on GMT day 220, 1988 showing received pulse shape after integration (top) and doppler spectrum (bottom) during a period of signal fading.

In the following, data taken from ALTAIR in the operational deep-space track mode is compared to satellite beacon data taken through a one-way communication link from FLTSATCOM 4 to a receiver located near ALTAIR. First the ALTAIR data is discussed.

SECTION 3

ALTAIR DEEP-SPACE DATA

In this section, ALTAIR data collected during two periods of FLTSATCOM 4 observation during day 232 and 233 are presented. These two examples were obtained from extended deep-space track of FLTSATCOM 4 over periods of time about 6-10 minutes in duration. Normal track duration in the deep-space mode is on the order of a minute or less - just enough time to place the object in track and obtain a few metric measurements to update the NORAD data base.

During normal PEAK operations on the evening of day 232, six satellite tracks were accomplished, and all but the earliest showed some periods of fading, roughly ranging from moderate to strong in severity. (As of this writing we have not yet completed processing of the ALTAIR satellite-track data and therefore have not yet quantified the degree of scintillation severity.) In an effort to measure the effects of strong scintillation on space track operation, ALTAIR was reconfigured into its operational UHF deep-space track mode to collect the following data while observing the FLTSATCOM 4 satellite.

Figure 3 depicts some ALTAIR measurements made during deep-space operations on the evening of GMT day 232. The figure shows ALTAIR data for the time period from 9.86 hours (9:52 P.M. local time) through about 10.07 hours (10:04 P.M.) in the early evening. In this figure ALTAIR measurements of azimuth, elevation, signal-to-noise ratio (SNR), radar cross section (RCS), and spectral width are shown. The values of elevation and azimuth are obtained from the radar track filter, while the values of RCS and SNR are measured at the peak of the output of the 512 pulse integration filter described above. Using ALTAIR-resident software, the spectral width is obtained as the second moment of the measured spectrum, where the range of the integration over doppler depends on the relative power of the outlying peaks in the measured spectrum.

The data shown in Figure 4 were taken the following evening (day 233) during a period of little or no ionospheric activity. A comparison of Figures 3 and 4 shows the effect of fading on the received signal after the coherent integration processing is completed.

In Figure 3, during a period of intense scintillation (as will be shown later through an examination of the one-way satellite link data), there is rapid variation

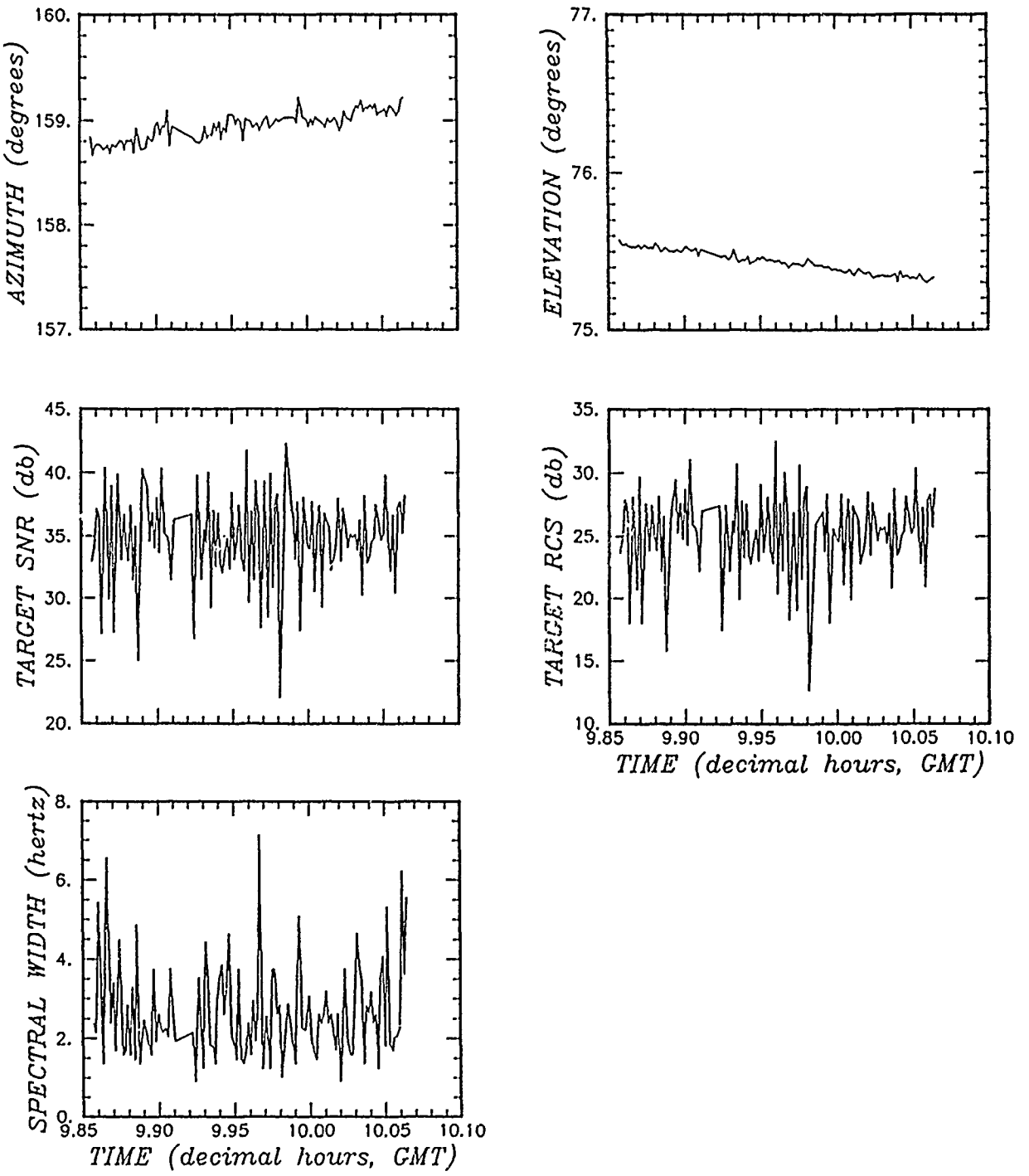

Figure 3. Summary of ALTAIR deep-space data collected during track of FLTSATCOM 4, GMT day 232, 1988 under disturbed ionospheric conditions.

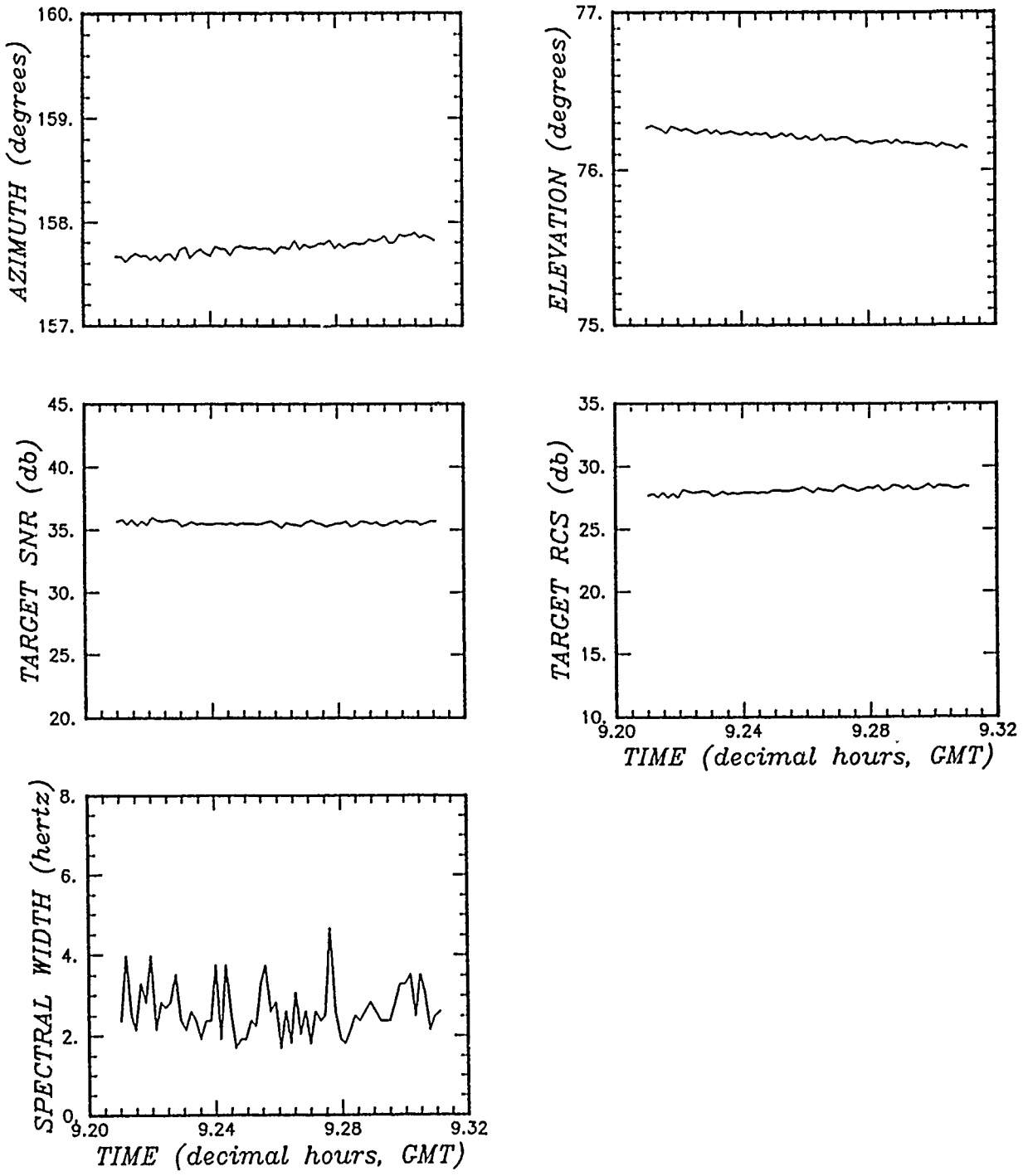

Figure 4. Summary of ALTAIR deep-space data collected during track of FLTSATCOM 4, GMT day 233, 1988 during quiet ionospheric conditions.

(scintillation) in received SNR and measured RCS with fades up to and exceeding 10 dB and many peaks (or foci) exceeding 5 dB above the average. The measured spectral width is often greater than 5 Hz and generally exhibits more variation than that shown in Figure 4. In addition, it appears that the measured azimuth shown in the upper left-hand corner of the two figures shows greater variability during the period of scintillation, while there is little fluctuation in elevation angle whether or not scintillation is present.

In Figure 4, during the period of little ionospheric activity, there is little or no fluctuation in RCS or SNR; the ALTAIR measured spectral width is generally less than 4 Hz and the measured elevation and azimuth angles are varying slowly to reflect the motion of the satellite (which takes the form of a figure eight in the reference frame of the rotating earth).

Figure 5 shows the cumulative probability distribution function of received power for the data shown in Figure 3. To provide a comparison to theoretical predictions, also plotted in the figure are several analytic curves appropriate to the Nakagami-*m* distribution. The analytic curves are identified by the value of S_4 appropriate for the one-way propagation path.

In a definitive paper *Fremouw, et al.*, [1980] utilized measurements of satellite link data to show that the Nakagami-*m* distribution is clearly superior to the log-normal, the generalized Gaussian and the two-component Gaussian distribution to describe the probability density function of the received power for the case of radio wave scattering by the ionosphere. This conclusion is based on a comprehensive analysis of the large body of scintillation data collected during the DNA Wideband Satellite experiment.

The measured cumulative distribution is shown by the short curve denoted by the value of S_4 of 0.33. This value is appropriate for the one-way propagation path; the actual measured value of S_4 was 0.67 which, of course, was measured after propagation on the two-way path from ALTAIR to FLTSATCOM 4 and back. Although there is only one curve representing less than 100 data points, it is apparent that the cumulative distribution of power agrees reasonably well with the predicted Nakagami-*m* distribution function.

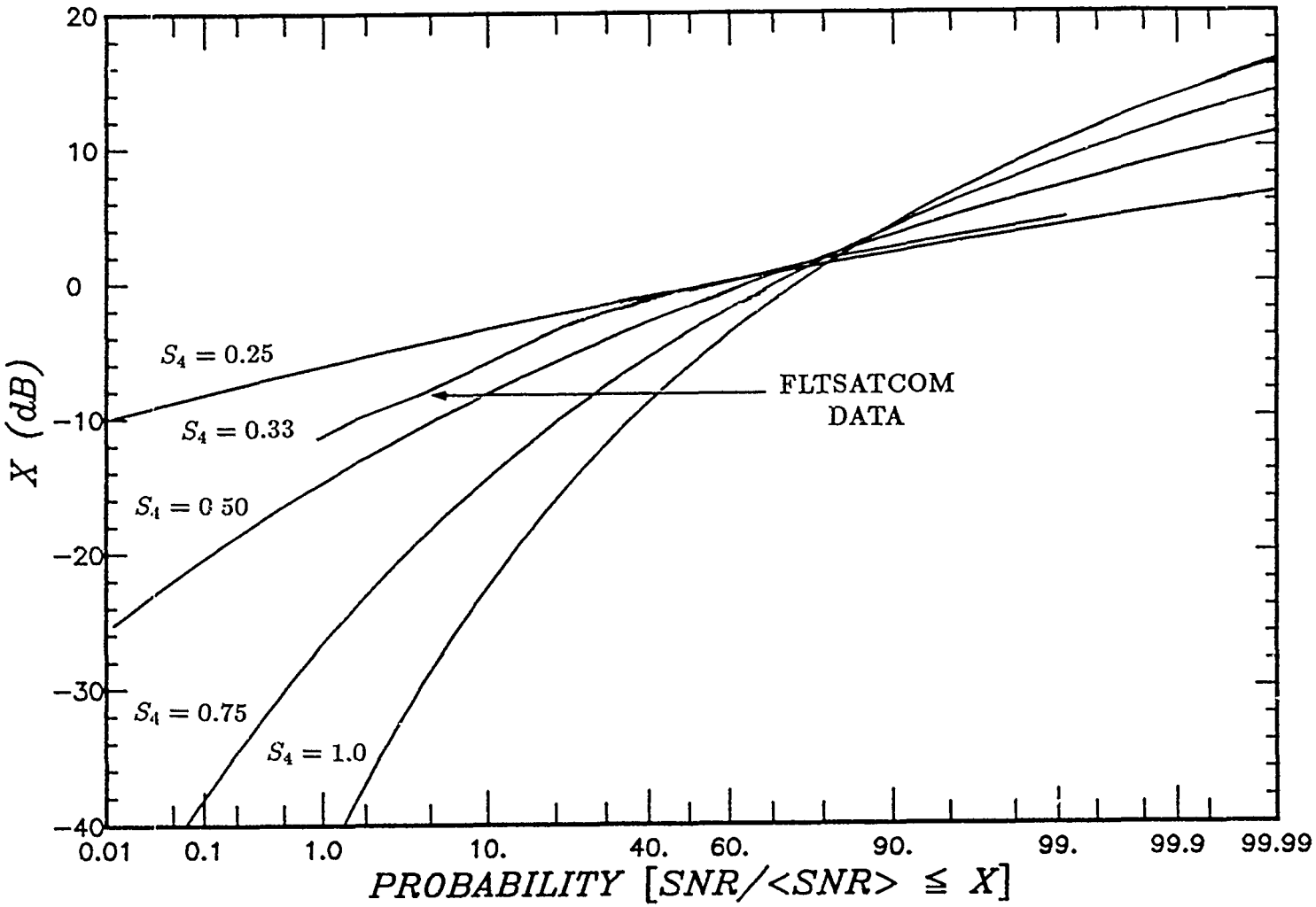

Figure 5. The cumulative probability distribution of received signal-to-noise ratio from FLTSATCOM 4 as measured during ALTAIR deep-space track.

SECTION 4

FLTSATCOM 4 SATELLITE LINK DATA

During the evenings of GMT days 232 and 233, the SRI FLTSATCOM receiver was monitoring a CW signal transmitted from Stanford, California to the geostationary FLTSATCOM 4 satellite. The assigned uplink frequency was 317.180 MHz and the phase-stable signal was transmitted using a 60-ft steerable dish antenna. Because there is little scintillation at mid-latitudes the uplink signal is undisturbed by ionospheric effects. The signal was regenerated on the satellite at a downlink frequency of 244.080 MHz. From Roi-Namur the downlink was received at a nominal elevation angle of 78° in a southeasterly direction.

The FLTSATCOM 4 observations on the evening of day 232 were characterized by pervasive scintillation; however, no scintillation was observed on day 233 which will be discussed no further.

Figures 6-8 show the received amplitude and phase as a function of time during various portions of the evening. Figure 6 shows a snapshot of the brief time period corresponding to the ALTAIR deep-space data described previously. It is seen that at the 244 MHz UHF frequency of FLTSATCOM, there are many occurrences of deep fades, often exceeding 20 dB. This figure also shows rapid phase scintillation that is always associated with amplitude fading, although the variations in phase are hard for the eye to detect during the large phase excursions shown here. Figure 7 shows the received amplitude and phase during the time period from 7.0 to 10.5 hours in the evening of GMT day 232. There are some unexplained (and unimportant) problems with the received signal early in the evening, but these have ended by 7:30 PM local time. Note the abrupt onset of scintillation at about 8.45 hours and the appearance of the patchy nature of equatorial plumes. The first patch ends at about 9.00 hours and the second ends at about 10.25 hours.

It is instructive to consider in detail some of the data taken from the FLTSATCOM 4 one-way link during the time period form 8.5 to 9.0 hours, at which time the first patch completes its passage through the line-of-sight. Figure 8 shows a detailed look at the received amplitude and phase during that period. During the beginning of this period the fade rate is quite rapid, but it is seen that the rapidity or fade rate of the scintillation (as measured by the amount of time between fades in the plot) is decreasing at the end of this period, between 8.9 and 9.0 hours. Although it is difficult to see, the occurrence of small, rapid phase variations also decreases somewhat

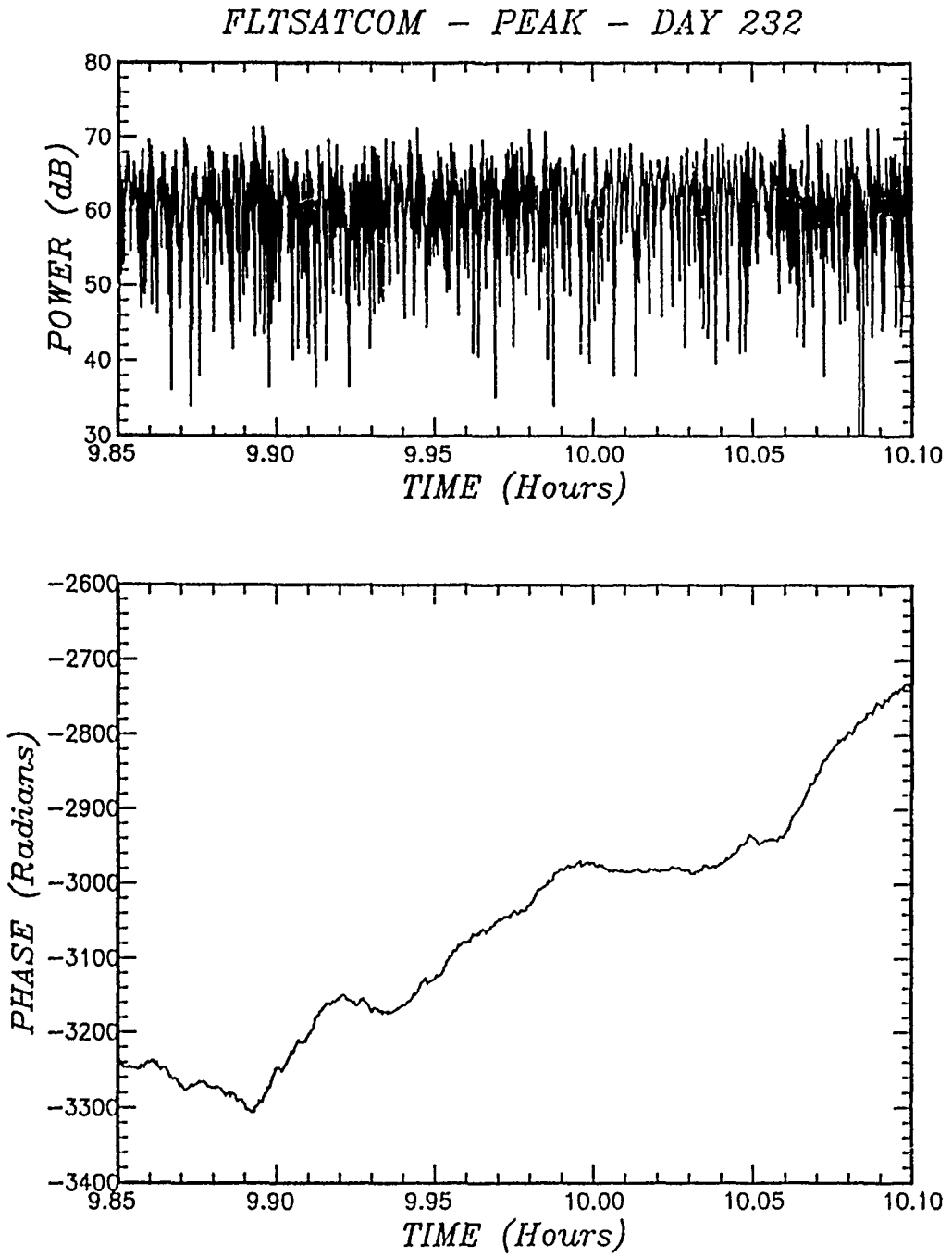

Figure 6. **Power and phase measured on the 244 MHz downlink from FLTSATCOM 4 on GMT Day 232, 1988, 9.85 to 10.1 hours GMT time.**

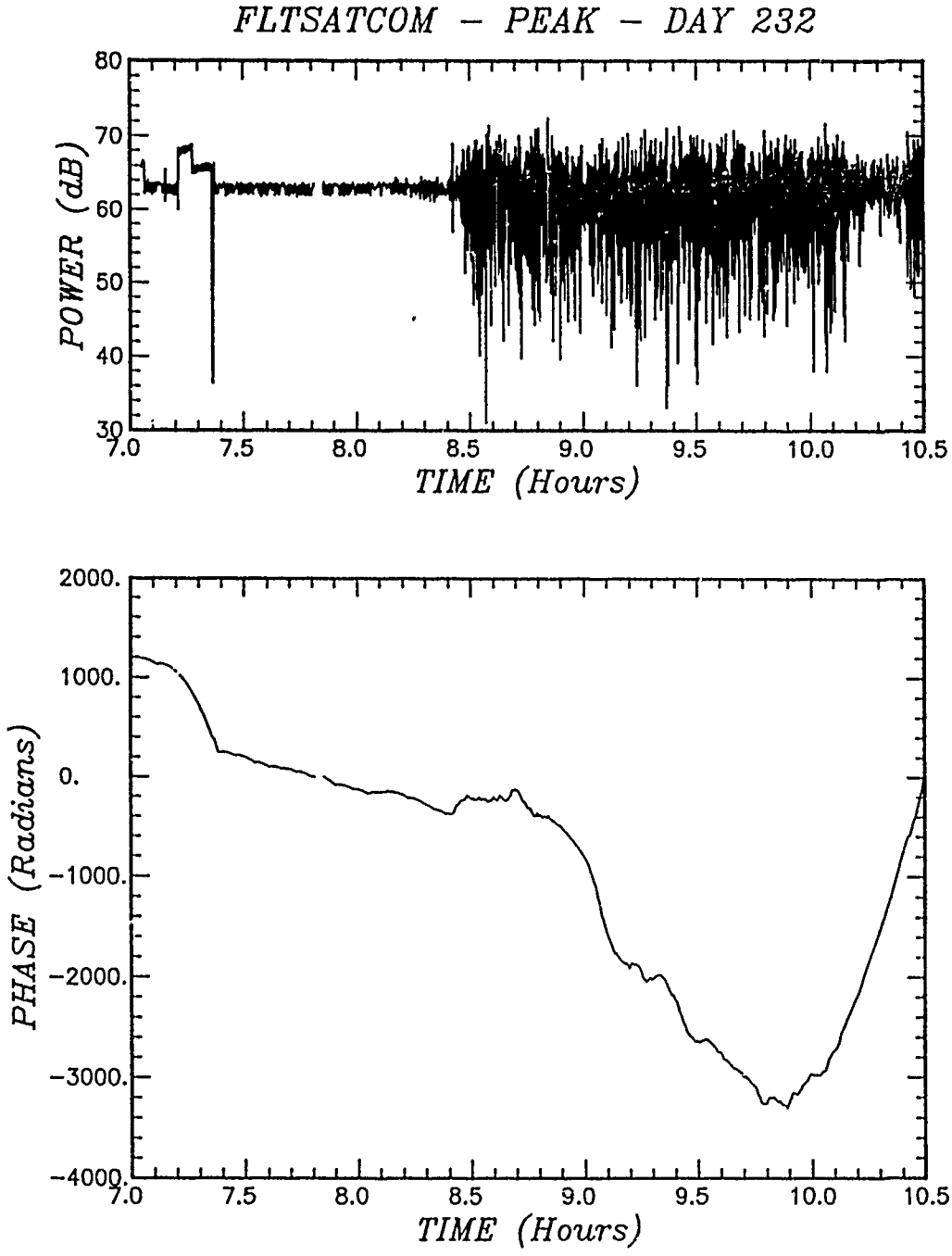

Figure 7. **Power and phase measured on the 244 MHz downlink from FLTSATCOM 4 on GMT Day 232, 1988, 7.0 to 10.5 hours GMT time.**

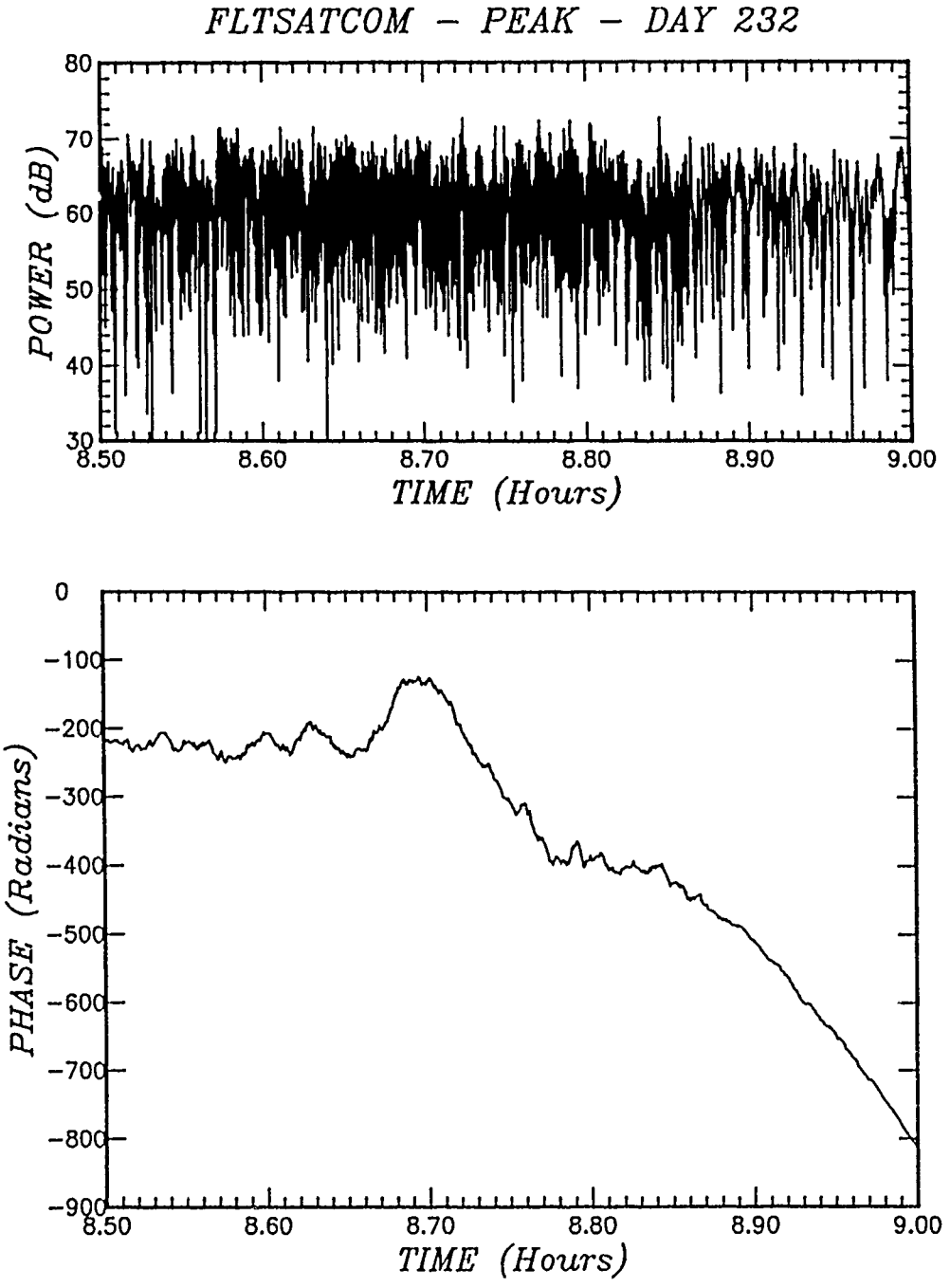

Figure 8. **Power and phase measured on the 244 MHz downlink from FLTSATCOM 4 on GMT Day 232, 1988, 8.5 to 9.0 hours GMT time.**

during this time. Phase variations indicate the presence of small-scale irregularities that cause signal scintillation. At the end of the 30 minute period of data shown in Figure 8, the scintillation has quieted as will be demonstrated through the computed doppler spectra to be discussed below.

Figures 9-11 show consecutive measurements of the doppler spectrum of the received signal. In each frame (except the last) there are 23 doppler spectra shown. The FLTSATCOM 4 data is recorded at a 100 Hz rate, corresponding to a doppler extent ranging from -50 to 50 Hz. To obtain each spectra, 512 successive samples of the complex received signal are Fourier transformed, corresponding to a total time duration of 5.12 seconds, or to a doppler resolution of 0.195 Hz. The complex Fourier transform is then multiplied by its complex conjugate to obtain the doppler spectrum. Only the central region, from -5 to 5 Hz is shown in the figures. In addition a threshold is applied to the plots so that any value below about 25 dB down from the peak value is plotted at the threshold value; this threshold is used for the plots only, and creates the straight lines shown in the figures.

The doppler spectra are plotted consecutively, one above the other, starting with the lower left hand corner of the figure. The ordinate is plotted in units of decibels, but the scale applies only to the lowermost plot of each frame. To plot all other spectra, multiples of 20 decibels were added to all ordinate values to achieve the separation of the individual spectra shown in these plots.

An examination of Figures 9-11 illustrates some important aspects of the effects of scintillation on radar coherent integration performance or, in other words, on radar doppler processing performance.

Space based radars, because of their long range requirements and limited onboard power per pulse, must coherently integrate the pulses in a coherent pulse-train (called a burst) in order to increase the signal-to-noise ratio and to reject clutter. Doppler processing essentially makes use of coherent integration to separate the radar return of a moving target from the large clutter return of the earth's surface. Since the earth is stationary, it occupies a different doppler bin than the moving target. Ground based radars must also use doppler processing if they are required to obtain range-doppler images for target discrimination purposes.

In either case the coherent integration process consists of the integration or summation of the complex signal from a number of consecutive pulses referred to as a burst. This is essentially identical to the Fourier transform process that is used here to obtain the doppler spectra that are shown in Figures 9-11.

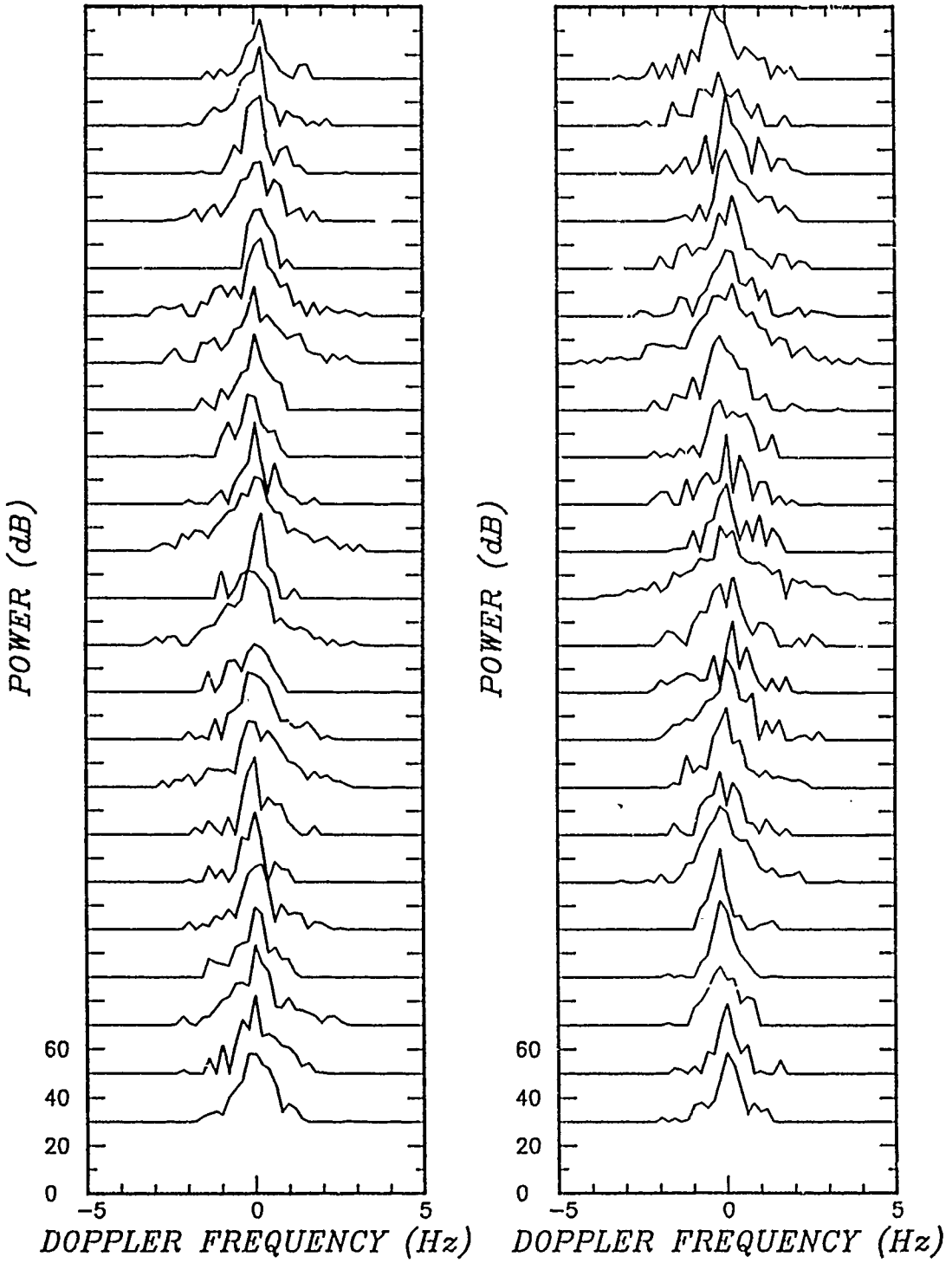

Figure 9. **Consecutive doppler spectra of the received FLTSATCOM signal corresponding to the time period from 8.503 to 8.567 hours GMT time.**

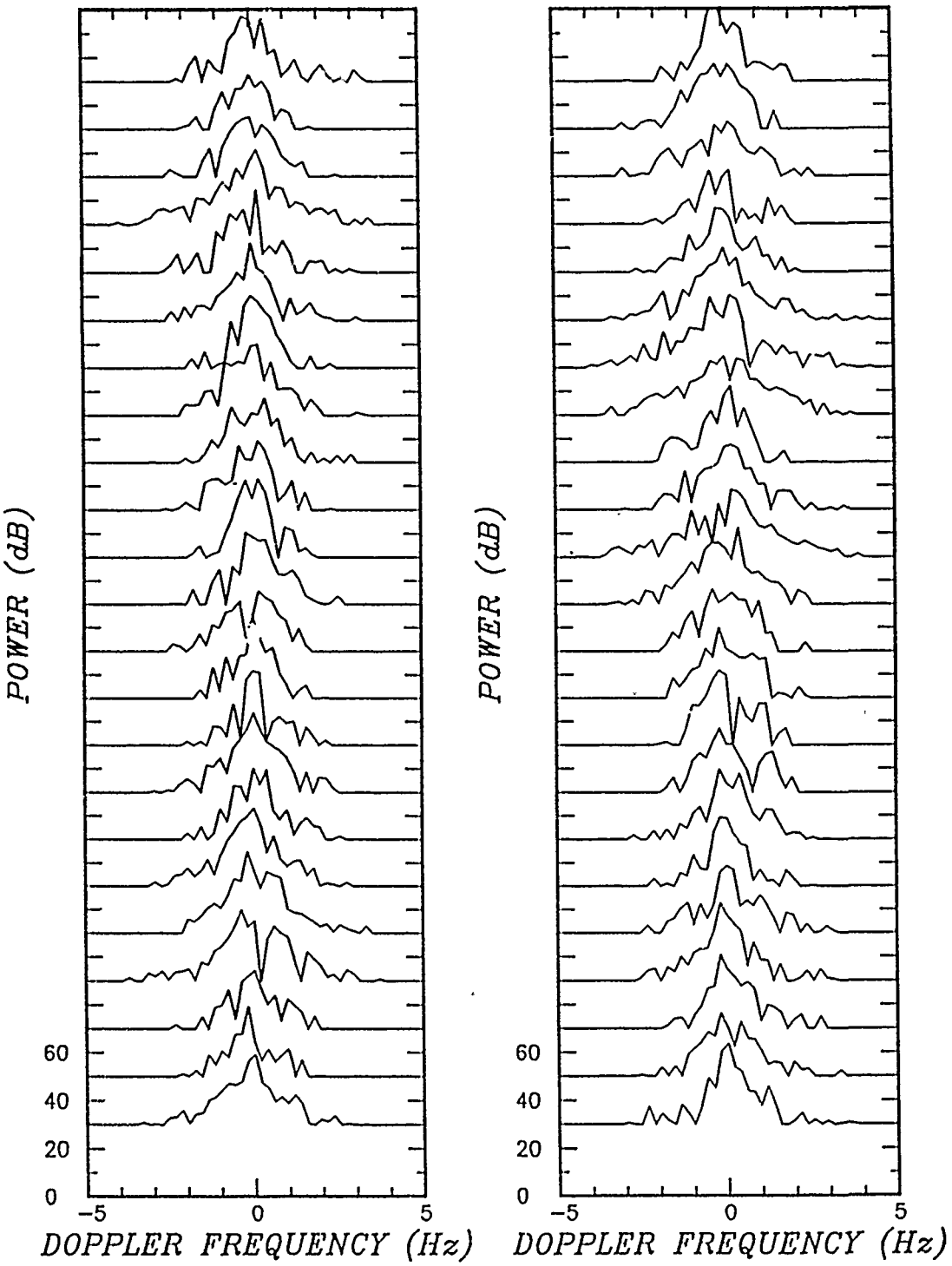

Figure 10. Consecutive doppler spectra of the received FLTSATCOM signal corresponding to the time period from 8.568 to 8.632 hours GMT time.

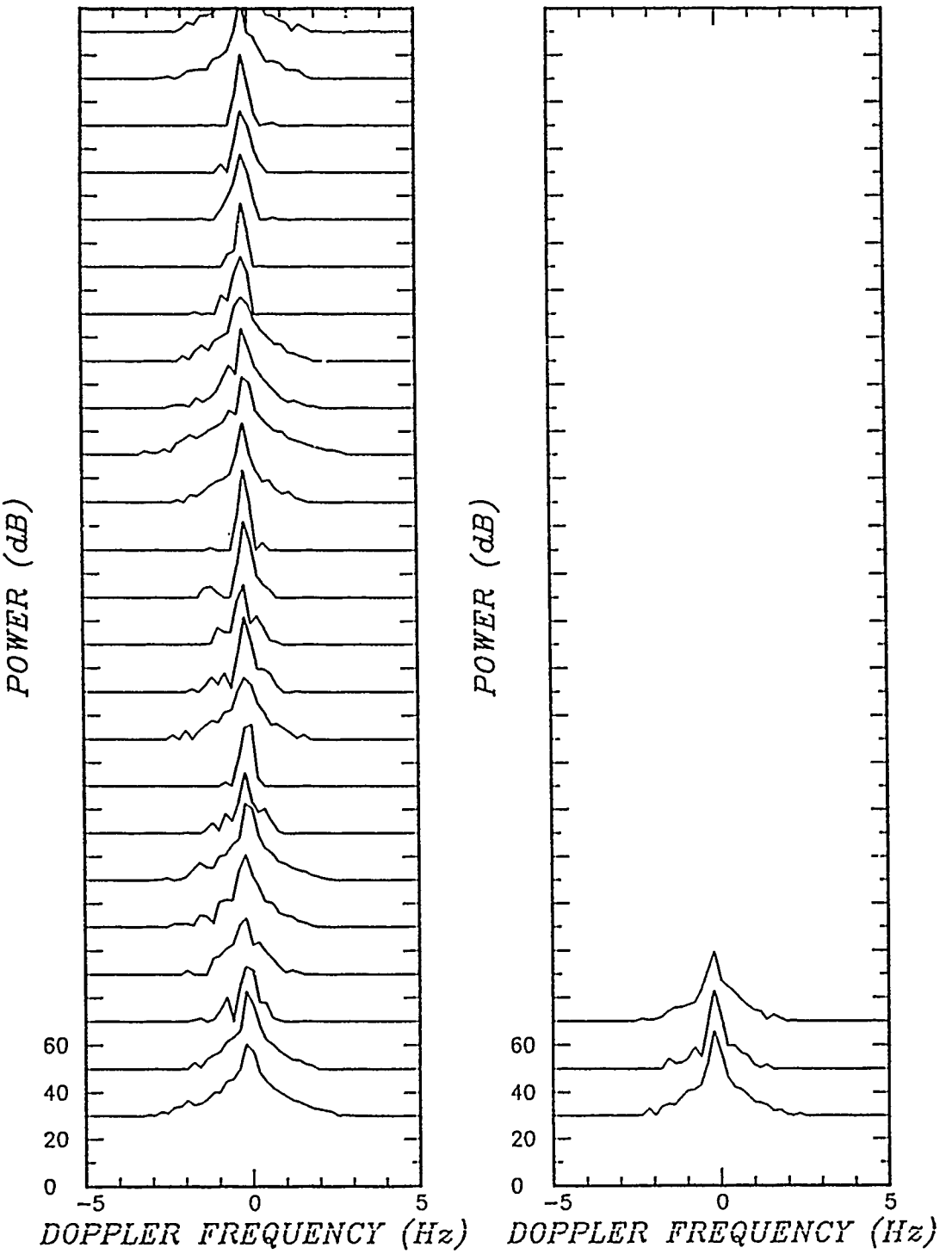

Figure 11. Consecutive doppler spectra of the received FLTSATCOM signal corresponding to the time period from 8.961 to 8.999 hours GMT time.

If the received signal is rapidly varying from pulse-to-pulse during the time duration of a burst, then we say that fast fading conditions prevail and there is a loss in the coherent integration process. This loss takes two forms. First, there is a spread in the doppler spectrum where energy spills over from the target doppler cell to other nearby doppler cells. This effect occurs when the bandwidth of the scintillation exceeds the doppler resolution of the coherent integration process. The second aspect of the degradation of the radar coherent integration process is the decrease in received energy in the desired target doppler bin, due to the spreading in doppler. This loss is referred to as coherent integration loss [*Knepp, Malokas, and Mokole*, 1988] and causes is a decrease in the peak achievable signal-to-noise ratio during scintillation.

Both types of degradation to coherent integration performance occur simultaneously as may be seen in Figures 9-11. In Figures 9-10, during the beginning of the 30 minute period selected for study, the scintillation is quite rapid in comparison to the 5.12 second coherent integration time used for the doppler processing, with the resulting spread in the doppler spectra shown. In Figure 11, at the end of the 30 minute period, the fading rate has decreased, and the received energy is concentrated in doppler with very little spreading.

The value of the coherent integration loss is a quantitative measure of the effect of fast fading on Space Radar coherent integration performance. It is defined as follows. The integration of a number of pulses, N, gives a voltage gain equal to the number of pulses and therefore a gain in output power of N^2. If there is fading from pulse-to-pulse during the time duration of the coherent burst, the net output power will be reduced below the desired value of N^2. The amount of this reduction in output power is referred to as the coherent integration loss. In this report a simple relationship between the measured coherent integration loss and the measured signal decorrelation time is shown to apply for the case of the severe fading on the FLTSATCOM 4 one-way link data. This result is then easily scaled to account for the loss in SNR observed in the ALTAIR deep-space track of FLTSATCOM during the same time period.

In the following the data taken from the one-way communication link from FLTSATCOM 4 to the SRI receiver on Roi-Namur during GMT day 232 is analyzed. Values of the S_4 scintillation index, the mean doppler, the doppler spread, and the signal decorrelation time are obtained. A simple method is presented to obtain the value of τ_0, the signal decorrelation time.

The received one-way propagation link data is then converted to the effective two-way monostatic radar geometry (through squaring of the received complex voltage) and the coherent integration loss is obtained as a function of the signal decorrelation time.

Figure 12 shows the average power and mean doppler of the received FLTSATCOM 4 signal during the evening of GMT day 232. The average power is obtained as the mean of 4096 samples corresponding to a 40.96 second average. The mean doppler is computed as the centroid frequency of a 40.96 second-duration FFT. Note the large variations in doppler that begin simultaneously with the onset of scintillation at 8.4 hours.

Figure 13 shows the S_4 scintillation index and the signal decorrelation time of the measured one-way data. The scintillation index is computed as the normalized standard deviation of the received power from the expression

$$S_4^2 = \frac{\langle P^2 - \langle P \rangle^2 \rangle}{\langle P \rangle^2} = \frac{\langle P^2 \rangle - \langle P \rangle^2}{\langle P \rangle^2} \tag{1}$$

where P is the received power and the angle brackets denote the average of the bracketed quantity over 4096 consecutive samples.

Figure 14 illustrates the important steps used in the measurement of the decorrelation time of the received FLTSATCOM 4 complex signal. The signal decorrelation time is defined as the time corresponding to the e^{-1} point of the autocorrelation function of the received complex signal. However the received signal spectrum corresponding to a Gaussian autocorrelation function is also Gaussian. Hence it is straightforward to establish a relationship between the doppler spread of the received spectrum and the value of the signal decorrelation time.

Given this relationship (shown in Figure 14) between doppler spread and signal decorrelation time, it is then necessary to measure only the doppler spread. To obtain the doppler spread σ_f, it is straightforward to compute the required spectral moments as indicated in the figure.

In our measurements of the moments of the signal spectrum, the summation was terminated whenever the value of energy in two consecutive doppler cells was more than 20 dB below the peak value of a particular doppler spectra. This procedure helps to reduce the effects of noise in the evaluation of the second moment of doppler.

Figure 15 shows the measured values of doppler spread, from which the measured values of τ_0 shown in the previous figure were obtained. Note the increased doppler spread and decreased signal decorrelation time during the period between 8.5 to 8.8 hours. From Figure 14, during the period of interest to the ALTAIR deep-space measurements, between 9.85 to 10.1 hours, the value of τ_0 ranges between 0.6 to 2.5 seconds with the most likely value of roughly 0.9-1.0 seconds.

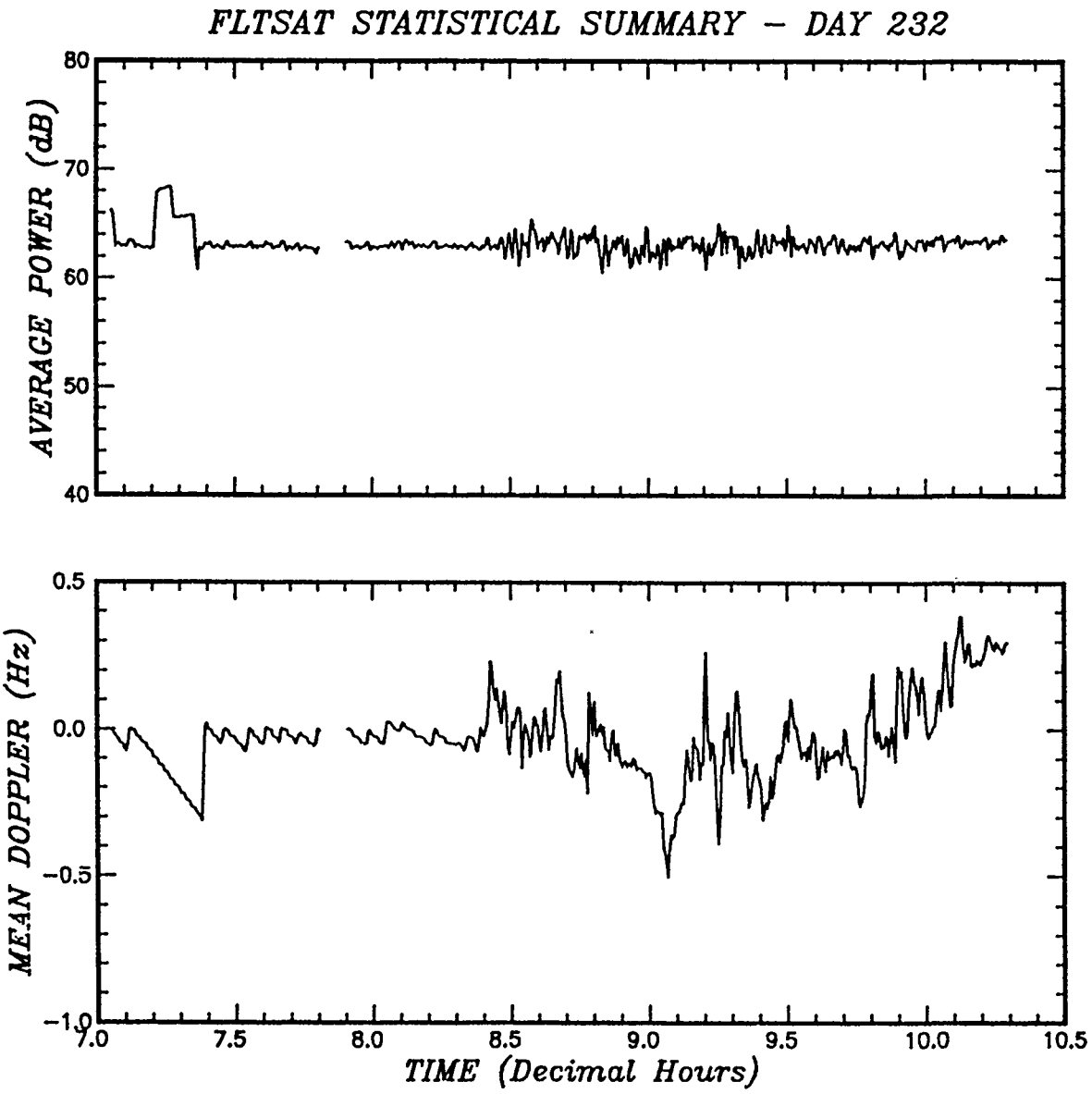

Figure 12. The average power and mean doppler of the received FLTSATCOM 4 signal as a function of time during the early evening of GMT day 232.

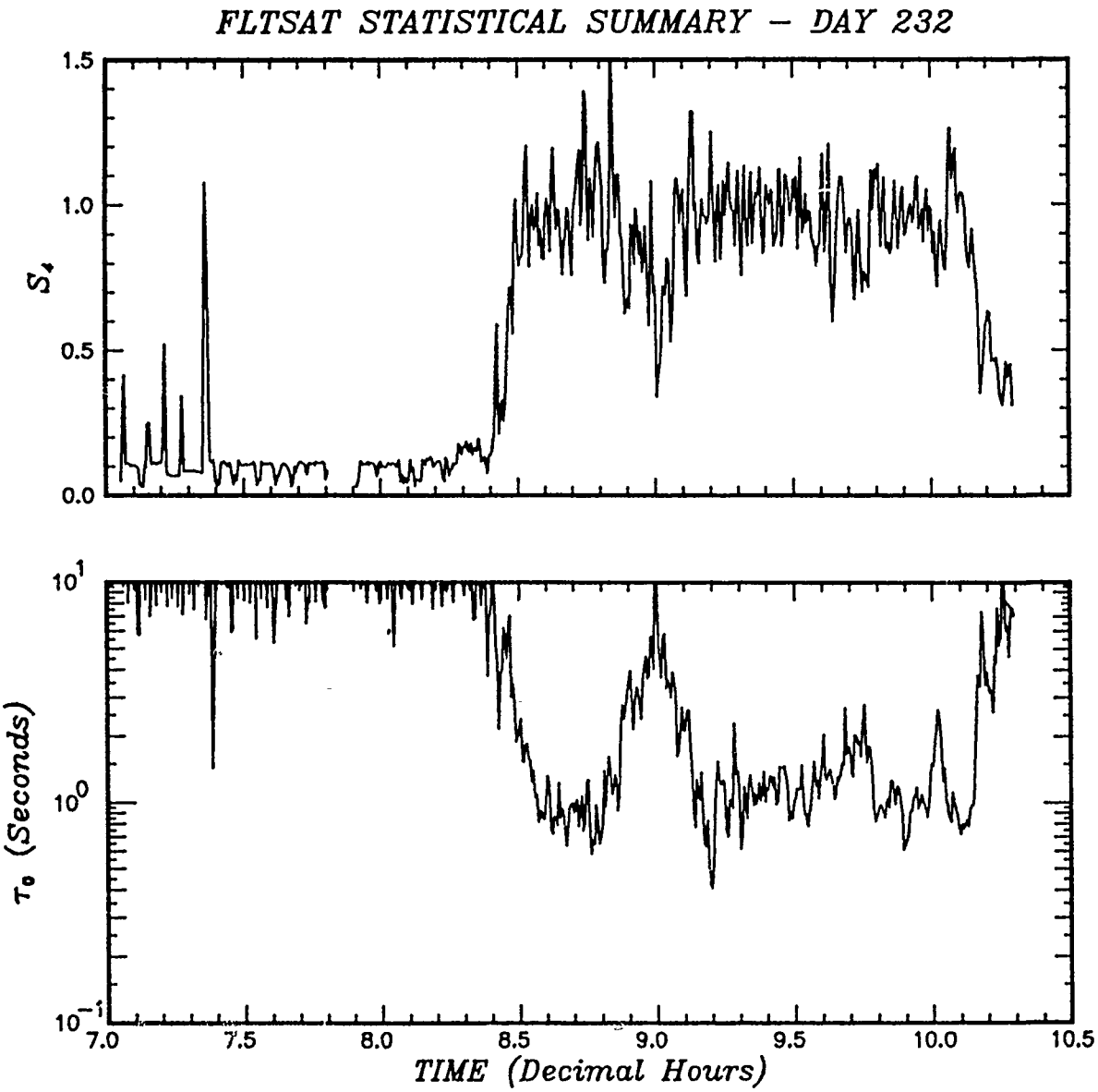

Figure 13. Measured values of scintillation index and signal decorrelation time as a function of time during the early evening of GMT day 232.

$$\rho(\tau) = |E_0|^2 \exp(-\tau^2/\tau_0^2)$$

$$S(f) = \frac{|E_0|^2}{\sqrt{2\pi}\sigma_f} \exp(-f^2/2\sigma_f^2)$$

$$\tau_0 = \frac{1}{\sqrt{2}\pi\sigma_f}$$

MEASURE σ_f AS:

$$\sigma_f^2 = \frac{1}{P}\sum_i f_i^2 S(f_i) - \left\{\frac{1}{P}\sum_i f_i S(f_i)\right\}^2$$

$$P = \sum_i S(f_i)$$

WHERE THE SUMMATION IS OVER ALL DOPPLER BINS

Figure 14. The use of the Gaussian assumption to relate the measured doppler spread to the value of τ_0, the signal decorrelation time.

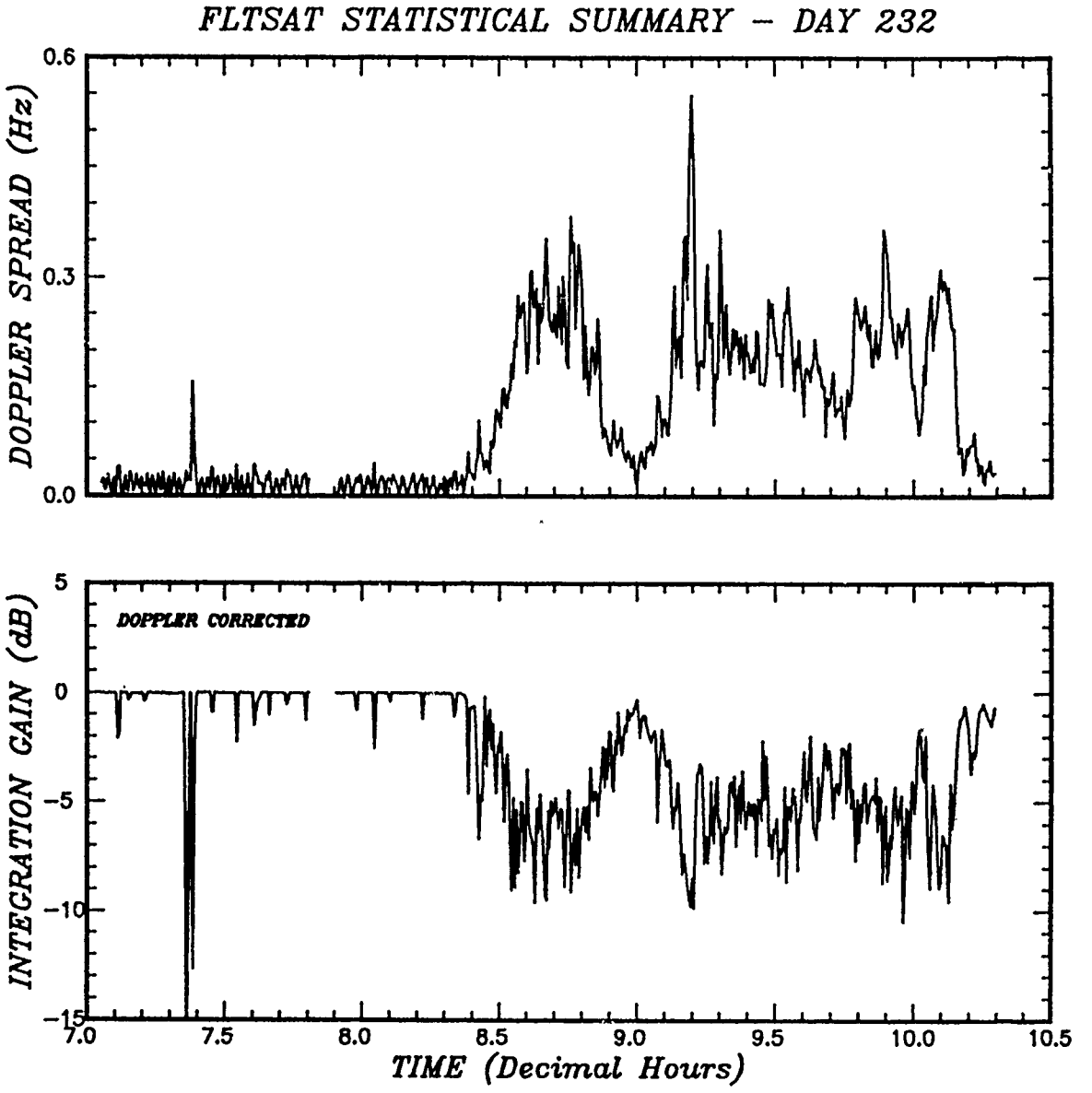

Figure 15. Measured values of doppler spread and coherent integration gain as a function of time during the early evening of GMT day 232.

To scale τ_0 from a one-way propagation path to a two-way path, decrease the value on the one-way path by a factor of $\sqrt{2}$. To scale to a higher frequency, increase τ_0 by the ratio of the frequencies [*Knepp and Reinking*, 1989]. Thus to transform a value of τ_0 measured at 244 MHz on a one-way link to the corresponding value for the ALTAIR two-way radar geometry at 422 MHz, multiply by the factor 1.22. Hence, if the propagation paths were identical (they are not) the most likely value of τ_0 for ALTAIR would range from 1.1-1.2 seconds. As shown later, this inferred range of values of τ_0 is consistent with the measured coherent integration loss.

4.1 FLTSATCOM 4 COHERENT INTEGRATION LOSS.

Figure 15 also shows the measured value of the normalized coherent integration gain corresponding to a hypothetical two-way radar link to FLTSATCOM 4 at a 244 MHz transmission frequency. This quantity is calculated as follows. First, the received one-way data (i.e., from the SRI receiver) is converted to the equivalent two-way radar data by squaring the complex received signal. In other words, the amplitude is squared and the phase is doubled. The generated two-way signal is then processed in the following manner. A burst is assumed to consist of 512 samples, each sample separated in time by 0.01 seconds. To obtain the quantity of interest, namely the coherent integration gain, 4096 samples of data over 40.96 seconds are divided into 8 bursts, each of which has a time duration of 5.12 seconds. The 512 complex samples in each burst are added and the resulting magnitude is obtained and divided by the average power per pulse times the number of pulses. Thus, if the pulse returns experience no scintillation during the burst duration, the results of this operation would by unity, or zero decibels. This process is repeated for all eight bursts corresponding to the 40.96 second duration and the average gain is computed and plotted in the figure.

As shown in Figure 15, decreases in coherent integration gain occur during scintillation with loss in gain (corresponding to a negative value of gain measured in decibels) occurring during conditions of increased doppler spread and decreased signal decorrelation time. It should be noted that the effect of shifts in the mean doppler have been removed prior to the calculation of the coherent integration gain shown in Figure 15. For example, the effect of a moving target or a linear time variation in total electron content would be to introduce a doppler offset in the measured spectrum. This shift in doppler could cause a decrease in peak power at the summation filter output unless the doppler shift was first removed from the phase of all the pulses in each burst. To obtain the values of coherent integration gain shown here, the mean doppler shift was removed from the complex signal prior to the coherent summation.

Figure 16 shows the relationship between the coherent integration loss (which is the inverse of the coherent integration gain) and the signal decorrelation time. The dots in the figure are the values measured with FLTSATCOM 4 data over the entire interval form 7.0 hours to 10.5 hours GMT time, day 232. As discussed previously, the measured one-way values of τ_0 have been scaled to two-way values by division by $\sqrt{2}$ and the complex voltage has been squared prior to calculation of the coherent integration loss to represent a monostatic radar geometry.

The solid curve shown in the figure is the analytic relationship between the ordinate and abscissa [*Dana and Knepp*, 1983; *Knepp, Malokas and Mokole*, 1988] under the assumption of strong scattering. The analytic curve is valid when the scintillation statistics on the one-way propagation path are strictly Rayleigh, with uncorrelated in-phase and quadrature components and with a Gaussian power spectrum. In spite of these analytic requirements the experimental results from the "two-way" FLTSATCOM 4 data closely match the analytic curve.

4.2 ALTAIR COHERENT INTEGRATION LOSS.

Now let us use the analytic curve, which gives a good match to the data, to infer the amount of coherent integration loss that was experienced during the period from 9.85 to 10.10 hours on GMT day 232. As the first step in this process determine the appropriate range of values of τ_0 at 244 MHz during this period, then utilize the analytic curve to determine the loss experienced by ALTAIR. As discussed above, the value of τ_0 during the time period from 9.85 to 10.10 hours ranges from 0.6 to 2.5 seconds with most values in the range from 0.9 to 1.0 seconds. To convert these one-way values measured at 244 MHz to two-way values at 422 MHz, multiply by the factor 1.22. This yields a range of values of τ_0 for ALTAIR of 0.73 to 3 seconds with a most likely range of 1.1 to 1.22 seconds.

Now in the deep-space track mode ALTAIR is usually coherently integrates 512 pulses over a time period of about 5 seconds per burst. Thus the ratio τ_0/T_{CI} will range from 0.15 to 0.6, with a most likely range of 0.22 to 0.24. Use of the analytic curve given in Figure 14 gives corresponding values of the coherent integration loss of 6.5 to 1.5 dB with a most likely range of loss between 4 to 4.5 dB. This calculation of 4-4.5 dB agrees quite well with the received ALTAIR data presented in Figure 3. Also note from the cumulative probability distribution presented in Figure 5, that 15 percent of the time, the received SNR is more than 4 dB below the average value during the brief time period of ALTAIR deep-space operation discussed here.

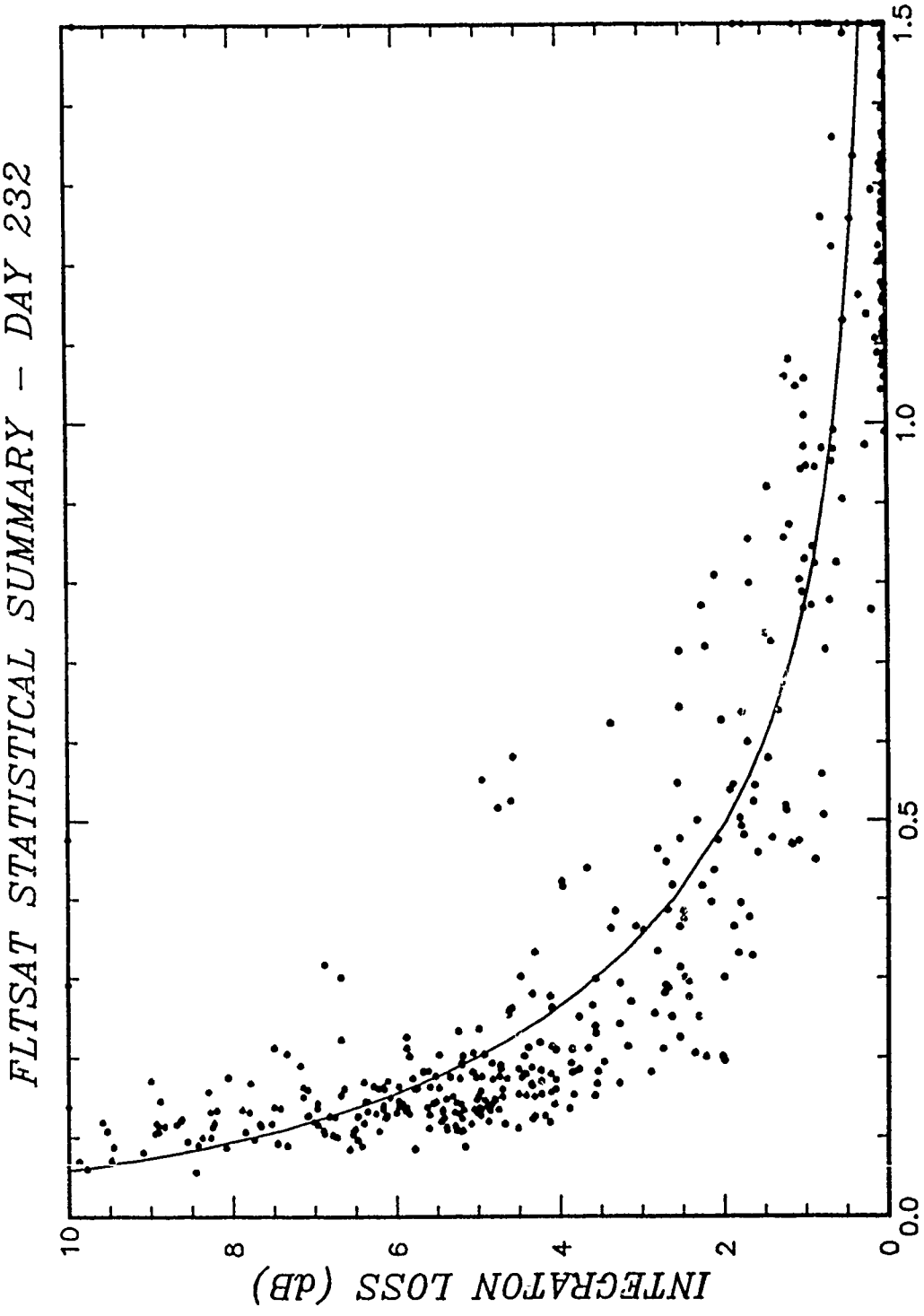

Figure 16. Two-way coherent integration loss versus the ratio of signal decorrelation time to coherent integration time, τ_0/T_{CI}.

SECTION 5

CONCLUSIONS

This report describes a brief period of time during the early evening of GMT day 232, August 1988 when the ALTAIR UHF deep-space track experienced measurable amounts of degradation due to signal scintillation caused by ionospheric irregularities. During this brief observation period, ALTAIR experienced specific instances of fading of more than 5 dB while tracking the FLTSATCOM 4 synchronous satellite. Simultaneous complementary measurements taken through a satellite communications down-link from FLTSATCOM 4 to a receiver located on Roi-Namur are analyzed in this report and are shown to collaborate the loss experienced by ALTAIR.

Because of the operational requirements of deep-space track, such scintillation currently does not seriously degrade ALTAIR performance. However, if ALTAIR requirements were to be changed to demand time-sensitive measurements of a low cross-section target where coherent integration is a necessity, then rapid scintillation could present operational difficulties.

In addition, current mitigation techniques (as of the August 1988 time frame) that automatically invoke additional pulses per burst when the coherent integrator output SNR is deemed to be too low are not optimal in dealing with fast fading. A better mitigation technique would be to reduce the coherent integration time to be consistent with the limitations imposed by the fading ionospheric channel and utilize additional amounts of non-coherent combining.

SECTION 6

LIST OF REFERENCES

Knepp, D. L., J. T. Malokas and E. Mokole, Space Radar Coherent Processing Performance During Scintillation, Mission Research Corporation Report MRY-R-011, Naval Research Laboratory Contract Number N00014-87-C-2336, Draft Report, March 1988.

Knepp, D. L. and J. T. Reinking, "Ionospheric Environment and Effects on SBR Detection", in *Space-Based Radar Handbook*, Ed. by L. J. Cantafio, Artech House, 1989.

Dana, R. A. and D. L. Knepp, "The Impact of Strong Scintillation on Space Based Radar Design. I. Coherent Detection", IEEE Trans. Aero. Electron. Syst., Vol. AES-19, No. 4, pp. 539-549, July 1983.

Fremouw, E. J., R. C. Livingston and D. A. Miller, "On the Statistics of Scintillating Signals," *Journal of Atmospheric and Terrestrial Physics*, Vol. 42, pp. 717-731, 1980.

DISTRIBUTION LIST

DNA-TR-89-76

DEPARTMENT OF DEFENSE

US NUCLEAR CMD & CENTRAL SYST SUPPORT STAFF
ATTN: SAB H SEQUINE

ASSISTANT TO THE SECRETARY OF DEFENSE
ATOMIC ENERGY
ATTN: EXECUTIVE ASSISTANT

DEFENSE ADVANCED RSCH PROJ AGENCY
ATTN: DR MANSFIELD
ATTN: GSD R ALEWINE

DEFENSE COMMUNICATIONS AGENCY
ATTN: A320

DEFENSE COMMUNICATIONS ENGINEER CENTER
ATTN: CODE R410

DEFENSE INTELLIGENCE AGENCY
ATTN: DC-6
ATTN: DIR
ATTN: DT-1B
ATTN: RTS-2B
ATTN: VP-TPO

DEFENSE NUCLEAR AGENCY
ATTN: DFSP G ULLRICH
ATTN: NANF
ATTN: NASF
ATTN: OPNA
3 CYS ATTN: RAAE
ATTN: RAAE A CHESLEY
ATTN: RAAE A MARDIGUIAN
ATTN: RAAE G ULLRICH
ATTN: RAAE M CRAWFORD
ATTN: RAAE S BERGGREN
ATTN: RAEE
4 CYS ATTN: TITL

DEFENSE NUCLEAR AGENCY
ATTN: TDNM
2 CYS ATTN: TDTT W SUMMA

DEFENSE TECHNICAL INFORMATION CENTER
2 CYS ATTN: DTIC/FDAB

JOINT DATA SYSTEM SUPPORT CTR
ATTN: C-312 R MASON

JOINT STRAT TGT PLANNING STAFF
ATTN: JK (ATTN: DNA REP)
ATTN: JKCS, STUKMILLER
ATTN: JLWT (THREAT ANALYSIS)
ATTN: JPEM
ATTN: JPSS

NATIONAL SECURITY AGENCY
ATTN: B432 C GOEDEKE

STRATEGIC AND THEATER NUCLEAR FORCES
ATTN: DR E SEVIN
ATTN: DR SCHNEITER
ATTN: LC R DAWSON

STRATEGIC DEFENSE INITIATIVE ORGANIZATION
ATTN: EN
ATTN: EN LTC C JOHNSON
ATTN: PTN C GIESE
ATTN: PTP LTC SEIBERLING
ATTN: TN

THE JOINT STAFF
ATTN: J6

DEPARTMENT OF THE ARMY

ARMY LOGISTICS MANAGEMENT CTR
ATTN: DLSIE

HARRY DIAMOND LABORATORIES
ATTN: SLCIS-IM-TL (TECH LIB)

U S ARMY ATMOSPHERIC SCIENCES LAB
ATTN: DR F NILES
ATTN: SLCAS-AE-E
ATTN: SLCAS-AR DR H HOLT

U S ARMY COMMUNICATIONS R&D COMMAND
ATTN: AMSEL-RD-ESA

U S ARMY FOREIGN SCIENCE & TECH CTR
ATTN: DRXST-SD

U S ARMY MISSILE COMMAND/AMSMI-RD-CS-R
ATTN: AMSMI-RD-CS-R (DOCS)

U S ARMY NUCLEAR & CHEMICAL AGENCY
ATTN: MONA-NU

U S ARMY NUCLEAR EFFECTS LABORATORY
ATTN: ATAA-PL
ATTN: ATAA-TDC
ATTN: ATRC-WCC

U S ARMY STRATEGIC DEFENSE CMD
ATTN: CSSD-H-LS B CARRUTH
ATTN: CSSD-H-SA R BRADSHAW
ATTN: CSSD-H-SA/R SMITH
ATTN: CSSD-H-SAV
ATTN: CSSD-H-TT M POPE

U S ARMY STRATEGIC DEFENSE COMMAND
ATTN: BMDATC-R W DICKERSON

USA SURVIVABILITY MANAGMENT OFFICE
ATTN: SLCSM-SE J BRAND

DEPARTMENT OF THE NAVY

COMMAND & CONTROL PROGRAMS
ATTN: OP 941

JOINT CRUISE MISSILES PROJECT OFC (PM-3)
ATTN: JCMG-707

NAVAL AIR SYSTEMS COMMAND
ATTN: PMA 271

NAVAL ELECTRONICS ENGRG ACTVY, PACIFIC
ATTN: CODE 250 D OBRYHIM

NAVAL RESEARCH LABORATORY
ATTN: CODE 2000 J BROWN
ATTN: CODE 2627 (TECH LIB)
2 CYS ATTN: CODE 4100 H GURSKY
ATTN: CODE 4121.8 H HECKATHORN
ATTN: CODE 4183
ATTN: CODE 4701
ATTN: CODE 4720 J DAVIS
ATTN: CODE 4750 P RODRIGUEZ
ATTN: CODE 4780 B RIPIN
ATTN: CODE 4780 DR P BERNHARDT
ATTN: CODE 4780 J HUBA
ATTN: CODE 5300
ATTN: CODE 5326 G A ANDREWS
ATTN: CODE 5340 E MOKOLE
ATTN: CODE 8344 M KAPLAN

NAVAL SURFACE WARFARE CENTER
ATTN: CODE H-21

NAVAL TECHNICAL INTELLIGENCE CTR
ATTN: DA44

NAVAL UNDERWATER SYSTEMS CENTER
ATTN: CODE 3411, J KATAN

OFC OF THE DEPUTY CHIEF OF NAVAL OPS
ATTN: OP 654/STRAT EVAL & ANAL BR
ATTN: OP 941D
ATTN: OP 981N

SPACE & NAVAL WARFARE SYSTEMS CMD
ATTN: CODE 3101 T HUGHES
ATTN: PD 50TD
ATTN: PD50TD1 G BRUNHART
ATTN: PME 106-4 S KEARNEY
ATTN: PME-106 F W DIEDERICH

THEATER NUCLEAR WARFARE PROGRAM OFC
ATTN: PMS-42331F (D SMITH)

DEPARTMENT OF THE AIR FORCE

AFIA
ATTN: AFIA/INKD MAJ SCHROCK

AIR FORCE CTR FOR STUDIES & ANALYSIS
ATTN: AFCSA/SASC

AIR FORCE ELECTRONIC WARFARE CENTER
ATTN: LT M MCNEELY

AIR FORCE GEOPHYSICS LABORATORY
ATTN: J KLOUBACHAR
ATTN: SANTI BASU

AIR FORCE SPACE SYSTEMS DIVISION
ATTN: YA
2 CYS ATTN: YN

AIR UNIVERSITY LIBRARY
ATTN: AUL-LSE

HQ AWS, DET 3 (CSTC/WE)
ATTN: WE

SECRETARY OF AF/AQQS
ATTN: AF/RDQI

STRATEGIC AIR COMMAND/XRFS
ATTN: XRFS

WEAPONS LABORATORY
ATTN: NTCA
ATTN: NTN
ATTN: SUL

DEPARTMENT OF ENERGY

EG&G, INC
ATTN: D WRIGHT

LAWRENCE LIVERMORE NATIONAL LAB
ATTN: L-97 T DONICH

LOS ALAMOS NATIONAL LABORATORY
ATTN: D SAPPENFIELD
ATTN: D WINSKE
ATTN: J MALIK
ATTN: T KUNKLE

SANDIA NATIONAL LABORATORIES
ATTN: D HARTLEY

SANDIA NATIONAL LABORATORIES
ATTN: A D THORNBROUGH
ATTN: C S WILLIAMS
ATTN: CODE 9014 R BACKSTROM
ATTN: D DAHLGREN
ATTN: ORG 7112 C MEHL
ATTN: ORG 9114 W D BROWN
ATTN: SPACE PROJECT DIV
ATTN: TECH LIB

OTHER GOVERNMENT

CENTRAL INTELLIGENCE AGENCY
ATTN: OSWR/NED
ATTN: OSWR/SSD FOR L BERG

DEPARTMENT OF COMMERCE
ATTN: E MORRISON
ATTN: G REEVE
ATTN: J HOFFMEYER
ATTN: W UTLAUT

U S DEPARTMENT OF STATE
ATTN: PM/TMP

DEPARTMENT OF DEFENSE CONTRACTORS

AEROSPACE CORP
ATTN: A LIGHTY
ATTN: A MORSE
ATTN: B P PURCELL
ATTN: C CREWS
ATTN: C RICE
ATTN: G LIGHT
ATTN: I GARFUNKEL
ATTN: J KLUCK
ATTN: M ROLENZ

ANALYTICAL SYSTEMS ENGINEERING CORP
ATTN: SECURITY

ATLANTIC RESEARCH SERVICES CORP
ATTN: R MCMILLAN

ATMOSPHERIC AND ENVIRONMENTAL RESEARCH INC
ATTN: M KO

AUSTIN RESEARCH ASSOCIATES
ATTN: J THOMPSON

AUTOMETRIC INCORPORATED
ATTN: C LUCAS

BDM INTERNATIONAL INC
ATTN: L JACOBS

BERKELEY RSCH ASSOCIATES, INC
ATTN: J WORKMAN
ATTN: S BRECHT

BOEING CO
ATTN: G HALL

CALIFORNIA RESEARCH & TECHNOLOGY, INC
ATTN: M ROSENBLATT

CHARLES STARK DRAPER LAB, INC
ATTN: A TETEWSKI

COMMUNICATIONS SATELLITE CORP
ATTN: G HYDE

CORNELL UNIVERSITY
ATTN: D FARLEY JR
ATTN: M KELLY

ELECTROSPACE SYSTEMS, INC
ATTN: P PHILLIPS

EOS TECHNOLOGIES, INC
ATTN: B GABBARD
ATTN: W LELEVIER

GENERAL ELECTRIC CO
ATTN: ROBERT H EDSALL

GENERAL RESEARCH CORP INC
ATTN: J EOLL

GRUMMAN AEROSPACE CORP
ATTN: J DIGLIO

HSS, INC
ATTN: D HANSEN

INFORMATION SCIENCE, INC
ATTN: W DUDZIAK

INSTITUTE FOR DEFENSE ANALYSES
ATTN: E BAUER
ATTN: H WOLFHARD

J S LEE ASSOCIATES INC
ATTN: DR J LEE

JAYCOR
ATTN: J SPERLING

JOHNS HOPKINS UNIVERSITY
ATTN: C MENG
ATTN: J D PHILLIPS
ATTN: R STOKES
ATTN: T EVANS/BLDG 1W

KAMAN SCIENCES CORP
ATTN: DASIAC
ATTN: E CONRAD
ATTN: G DITTBERNER

KAMAN SCIENCES CORPORATION
ATTN: B GAMBILL
ATTN: DASIAC
ATTN: R RUTHERFORD

LOCKHEED MISSILES & SPACE CO, INC
ATTN: J HENLEY
ATTN: J KUMER
ATTN: R SEARS

LOCKHEED MISSILES & SPACE CO, INC
ATTN: D KREJCI

LTV AEROSPACE & DEFENSE COMPANY
2 CYS ATTN: LIBRARY

M I T LINCOLN LAB
ATTN: D TOWLE
ATTN: I KUPIEC
ATTN: M LEE

MARTIN MARIETTA DENVER AEROSPACE
ATTN: H VON STRUVE III
ATTN: J BENNETT

MAXIM TECHNOLOGIES, INC
ATTN: B RIDGEWAY
ATTN: J SCHLOBOHM

MCDONNELL DOUGLAS CORPORATION
ATTN: J GROSSMAN
ATTN: R HALPRIN

METATECH CORPORATION
ATTN: R SCHAEFER
ATTN: W RADASKY

METEOR COMMUNICATIONS CORP
ATTN: R LEADER

MISSION RESEARCH CORP
ATTN: R ARMSTRONG
ATTN: W WHITE

MISSION RESEARCH CORP
ATTN: B R MILNER
ATTN: C LONGMIRE
ATTN: D ARCHER
2 CYS ATTN: D KNEPP
ATTN: D LANDMAN
ATTN: F FAJEN
ATTN: F GUIGLIANO
ATTN: G MCCARTOR
ATTN: K COSNER
ATTN: M FIRESTONE
ATTN: R BIGONI
ATTN: R BOGUSCH
ATTN: R DANA
ATTN: R HENDRICK
ATTN: R KILB
ATTN: S GUTSCHE
ATTN: TECH INFO CENTER
ATTN: TECH LIBRARY

MITRE CORPORATION
ATTN: M HORROCKS
ATTN: R C PESCI
ATTN: W FOSTER

NORTHWEST RESEARCH ASSOC, INC
ATTN: E FREMOUW

PACIFIC-SIERRA RESEARCH CORP
ATTN: E FIELD JR
ATTN: F THOMAS
ATTN: H BRODE

PHOTOMETRICS, INC
ATTN: I L KOFSKY

PHOTON RESEARCH ASSOCIATES
ATTN: D BURWELL
ATTN: O LEWIS

PHYSICAL RESEARCH INC
ATTN: W SHIH

PHYSICAL RESEARCH INC
ATTN: H FITZ
ATTN: P LUNN
ATTN: W HEUSER

PHYSICAL RESEARCH, INC
ATTN: R DELIBERIS
ATTN: T STEPHENS

PHYSICAL RESEARCH, INC
ATTN: J DEVORE
ATTN: J THOMPSON
ATTN: W SCHLUETER

PHYSICS INTERNATIONAL CO
ATTN: C GILMAN

R & D ASSOCIATES
ATTN: C GREIFINGER
ATTN: F GILMORE
ATTN: G HOYT
ATTN: M GANTSWEG

RAND CORP
ATTN: C CRAIN
ATTN: E BEDROZIAN

RAND CORP
ATTN: B BENNETT

RJO ENTERPRISES/POET FAC
ATTN: A ALEXANDER
ATTN: W BURNS

SCIENCE APPLICATIONS INTL CORP
ATTN: S ROSENCWEIG

SCIENCE APPLICATIONS INTL CORP
ATTN: C SMITH
ATTN: D HAMLIN
ATTN: D SACHS
ATTN: E STRAKER
ATTN: L LINSON

SCIENCE APPLICATIONS INTL CORP
ATTN: D TELAGE
ATTN: M CROSS

SRI INTERNATIONAL
ATTN: R LIVINGSTON
ATTN: R T TSUNODA
ATTN: W CHESNUT
ATTN: W JAYE

STEWART RADIANCE LABORATORY
ATTN: R HUPPI

TELECOMMUNICATION SCIENCE ASSOCIATES
ATTN: R BUCKNER

TELEDYNE BROWN ENGINEERING
ATTN: J WOLFSBERGER, JR
ATTN: N PASSINO

TOYON RESEARCH CORP
ATTN: J ISE

TRW INC
ATTN: H CULVER

TRW SPACE & DEFENSE SYSTEMS
ATTN: D M LAYTON

USER SYSTEMS, INC
ATTN: S W MCCANDLESS, JR

UTAH STATE UNIVERSITY
ATTN: K BAKER
ATTN: L JENSEN

VISIDYNE, INC
ATTN: J CARPENTER

FOREIGN

FOA 2
ATTN: B SJOHOLM

FOA 3
ATTN: T KARLSSON

DIRECTORY OF OTHER

BOSTON UNIVERSITY
ATTN: MICHAEL MENDILLO